

Electronic Supporting Information for

**Digestion-on-a-chip: A Continuous-Flow Modular Microsystem
Recreating Enzymatic Digestion in the Gastrointestinal Tract**

Pim de Haan^{1,2}, Margaryta A. Ianovska^{1,2}, Klaus Mathwig¹, Glenn A.A. van Lieshout³,
Vassilis Triantis³, Hans Bouwmeester^{4,5}, and Elisabeth Verpoorte¹

- ¹ University of Groningen, Groningen Research Institute of Pharmacy, Pharmaceutical Analysis;
P.O. Box 196, XB20, 9700 AD Groningen, The Netherlands. Email: e.m.j.verpoorte@rug.nl.
- ² TI-COAST; Amsterdam, The Netherlands.
- ³ FrieslandCampina, Amersfoort, The Netherlands.
- ⁴ RIKILT – Wageningen UR; Wageningen, The Netherlands.
- ⁵ Wageningen University, Division of Toxicology; Wageningen, The Netherlands.

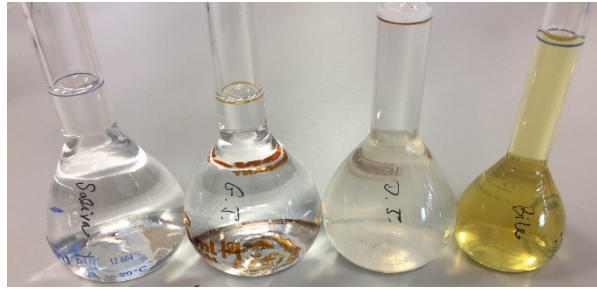


Figure S 1. Freshly prepared artificial digestive juices in volumetric flasks. Saliva and gastric juice are clear, but the duodenal juice and bile are somewhat turbid.

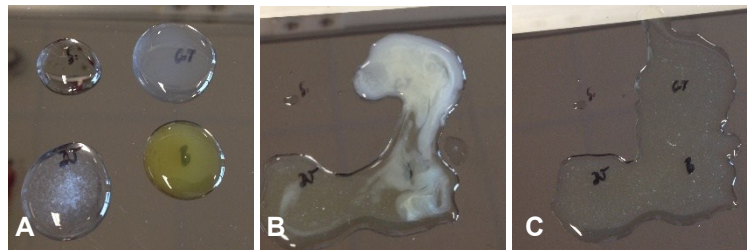


Figure S 2. Precipitations became visible upon mixing the four juices in the original composition (pre-optimization). A) Photo of the four juices separately, B) immediately after mixing and C) after 2 minutes of mixing. The precipitate seems to disappear after longer mixing. The same effect can be seen when mixing these juices on-chip, see Figure 4 in the main text.

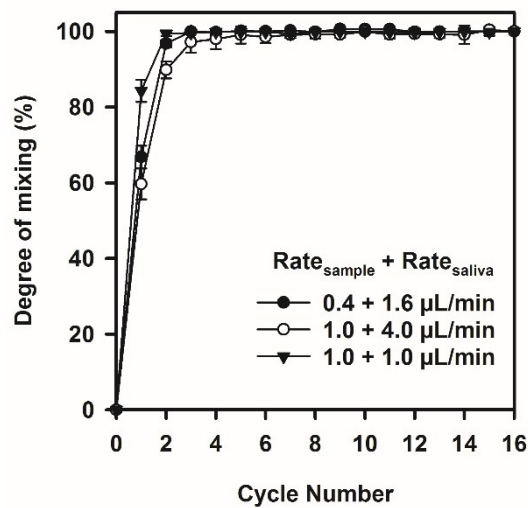


Figure S 3. Characterization of the mixing process of a sample ($5\mu\text{M}$ fluorescein in ultrapure water) with saliva, on-chip, at 37°C ($n = 3$, average \pm standard deviation). The mixing process is fast: at different flow rates and ratios, the mixing process is complete after 4 cycles (12.5 mm) in the channel for total flow rates of 2 and $5\mu\text{L}/\text{min}$ ($Re = 0.29$ and $Re = 0.72$; see ref.¹ for calculation of Reynolds numbers).

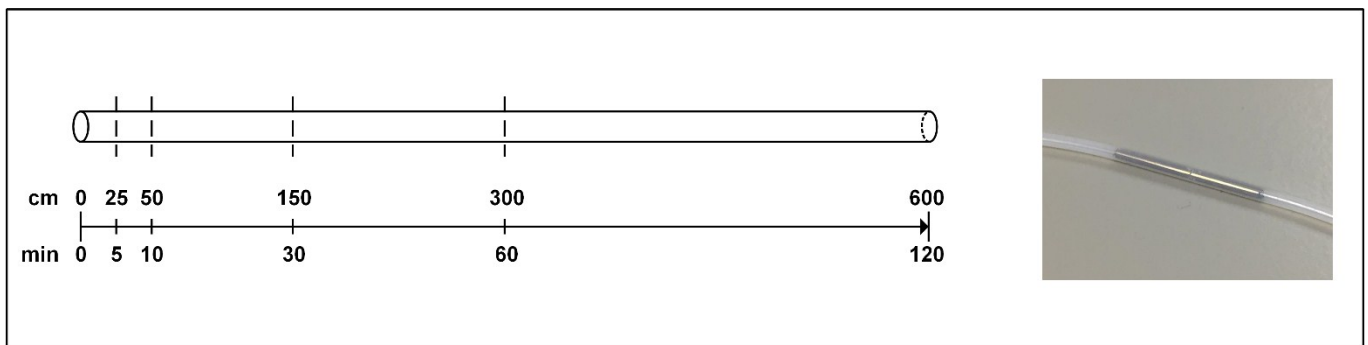


Figure S 4. Schematic representation of the incubation loop after the intestinal phase (see Figure 3 in main text). The tubing in this loop has been pre-cut at specific distances (with respective incubation times), to facilitate sampling. The pre-cut pieces of tubing are reconnected using blunt 21G needles (insert).

Optimizing the pH of Artificial Digestive Juices

The calculation of pH values of simple solutions, containing one acid or base at a certain concentration, is a straightforward process. When multiple acids, bases and amphiprotic species (both weak and strong) are mixed at the same time, a complex mixture arises in which multiple acid-base equilibria are valid at the same time. In such a situation, $[H^+]$ and the pH may be determined using acid dissociation, the water equilibrium (K_w), mass balances and electroneutrality.² Several computer-based tools have been developed to perform complex pH calculations, and one such program was used to perform these calculations (V. Vanovschi, pH solver, available: <http://www.webqc.org/phsolver.php>; accessed April–July 2018). It was found that other species present in the artificial digestive juices, *e.g.* sulfate and thiocyanate in saliva, have a negligible effect on the final pH. Therefore, only the species and acid dissociation constants listed in Table S 1 were used. Table S 2 and Table S 3 show the concentrations of species before optimization, based on work by Walczak *et al.*³, and after optimization, respectively. The pH values of 7.0, 3.0 and 7.0 in the consecutive compartments were chosen analogous to the work of Minekus *et al.*⁴ Values in red correspond to modified conditions to obtain an optimized pH.

Table S 1. Acid dissociation constants used to calculate the pH of juices and mixtures⁵.

	$pK_{a,1}$	$pK_{a,2}$	pK_b
HCl	-1		
OH ⁻			-1
H ₂ PO ₄ ⁻	7.198	12.375	11.852
HCO ₃ ⁻	10.329		7.649

Table S 2. Concentrations of species determining the pH of juices and mixtures *before optimization* (in mM), with the calculated $[H^+]$ and pH values.

Species	Sample	Saliva	Gastric Juice	Duodenal Juice	Bile	Oral Mixture	Gastric Mixture	Intestinal Mixture
HCl	0.00	0.00	99.60	2.16	2.40	0.00	61.29	32.95
OH ⁻	0.00	1.80	0.00	0.00	0.00	1.44	0.55	0.29
H ₂ PO ₄ ⁻	0.00	7.40	2.22	0.59	0.00	5.92	3.64	2.08
HCO ₃ ⁻	0.00	0.00	0.00	40.33	68.86	0.00	0.00	23.92
H ⁺ (M)	1.00×10^{-7}	1.97×10^{-7}	9.66×10^{-2}	3.09×10^{-8}	1.74×10^{-8}	1.97×10^{-7}	5.72×10^{-2}	7.64×10^{-3}
pH	7.000	6.705	1.015	7.510	7.760	6.705	1.243	2.117

Table S 3. Concentration of species determining the pH of juices and mixtures *after optimization* (in mM), with the calculated $[H^+]$ and pH values.

Species	Sample	Saliva	Gastric Juice	Duodenal Juice	Bile	Oral Mixture	Gastric Mixture	Intestinal Mixture
HCl	0.00	0.00	4.16	5.57	6.17	0.00	2.56	4.10
OH ⁻	0.00	2.90	0.00	0.00	0.00	2.32	0.89	0.46
H ₂ PO ₄ ⁻	0.00	7.40	2.22	0.59	0.00	5.92	3.64	2.08
HCO ₃ ⁻	0.00	0.00	0.00	40.33	68.86	0.00	0.00	23.92
H ⁺ (M)	1.00×10^{-7}	9.84×10^{-8}	3.44×10^{-3}	7.58×10^{-8}	4.44×10^{-8}	9.84×10^{-8}	1.16×10^{-3}	1.02×10^{-7}
pH	7.000	7.007	2.464	7.120	7.352	7.007	2.936	6.992

Raw Data of the Enzyme Assays

Alpha-amylase in saliva (mouth)

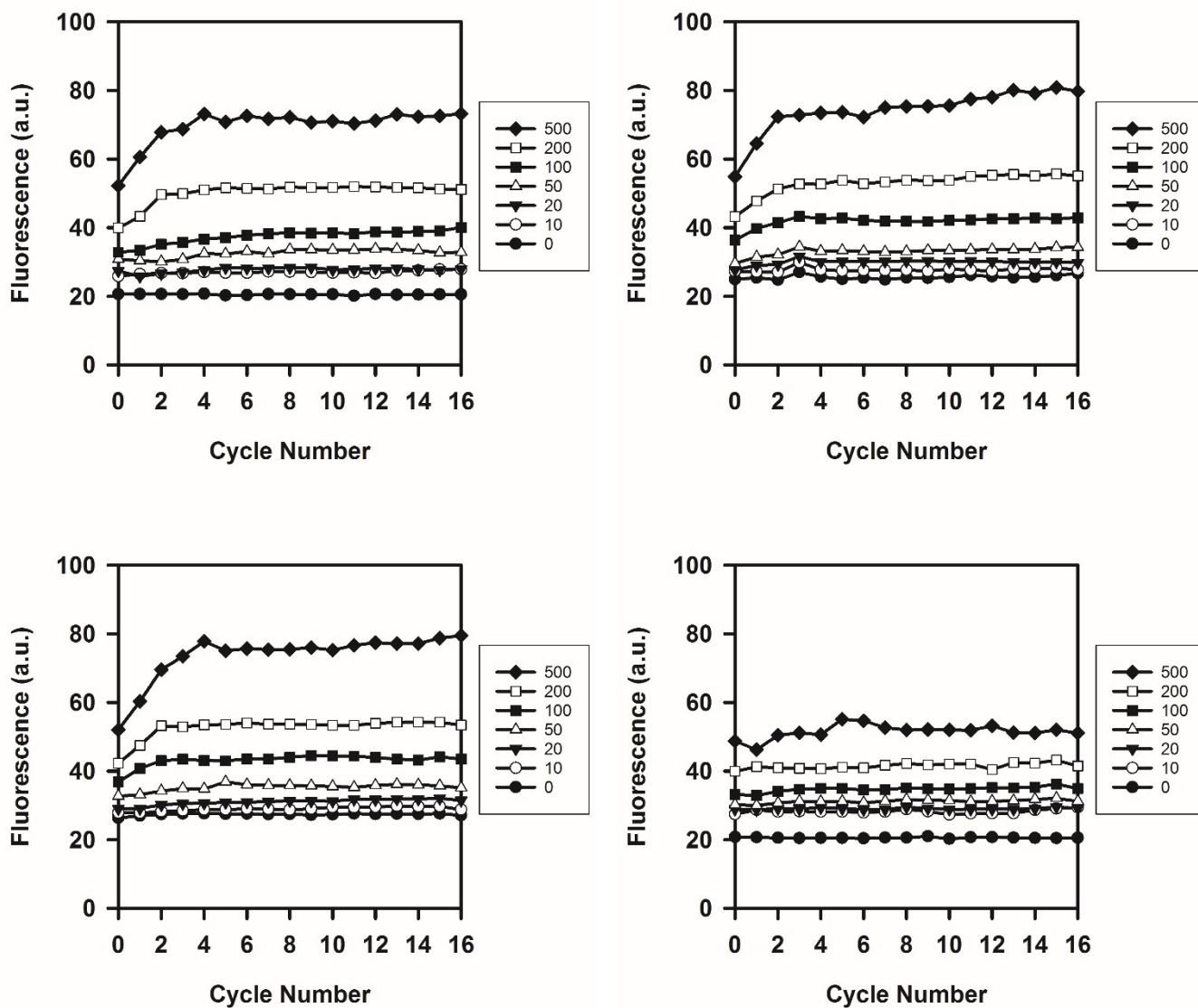


Figure S 5. On-chip fluorescence signals of the α -amylase-catalyzed digestion of starch plotted against the cycle number ($n = 3$, with the negative control containing no α -amylase at the bottom right). The legend displays [starch] in the substrate inlet ($\mu\text{g/mL}$).

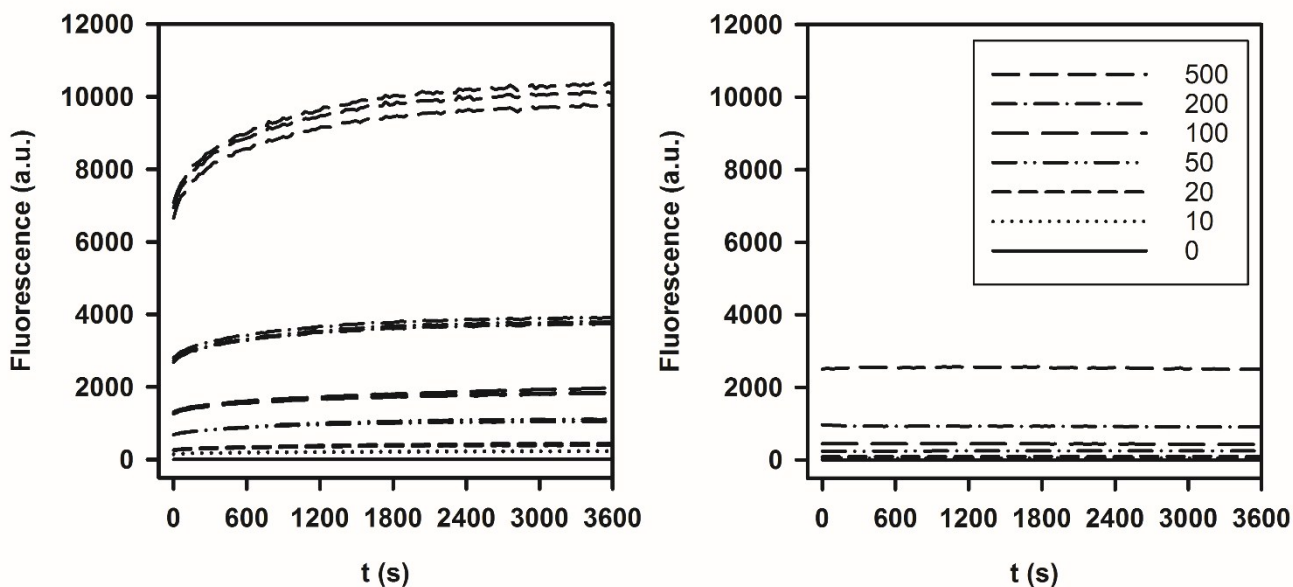


Figure S 6. α -amylase-catalyzed digestion of labeled starch, monitored by fluorimeter (left: with enzyme, $n = 3$; right: without enzyme). Substrate concentrations in the samples (before mixing 1:4 with saliva) are listed in $\mu\text{g/mL}$. The exact same conditions were used, compared to the conditions of on-chip experiments (same mixing ratio, same composition, 37°C).

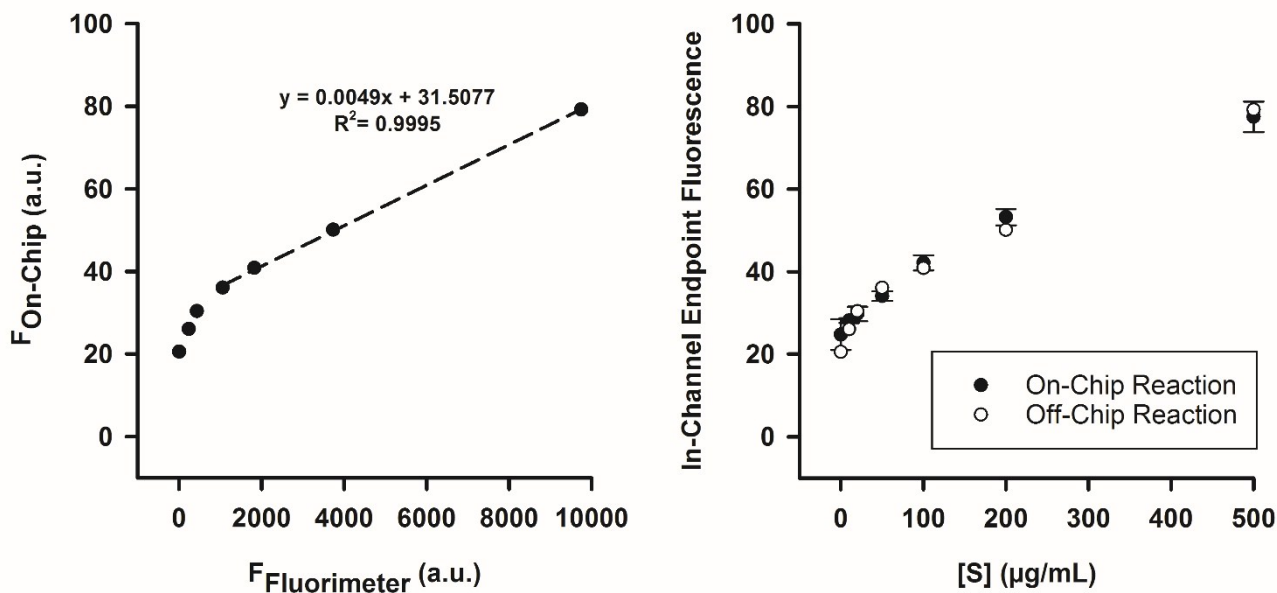


Figure S 7. After the fluorimeter-monitored reaction had progressed for 1 h (see Figure S 6), the reaction mixture was transferred to a microfluidic mixer to measure the fluorescent signal on-chip. Left: The endpoint fluorescence on-chip was plotted versus the fluorescence measured in the fluorimeter, yielding an excellent linear correlation at higher fluorescence values. Right: The endpoint fluorescence (measured on chip, after transferring the reaction mixture) of the reaction in plate plotted versus $[S]$, and the endpoint fluorescence of the identical reactions monitored on-chip, plotted versus $[S]$. In this way, we can compare the endpoint fluorescence of this off-chip reaction with the on-chip reaction. The endpoint fluorescence of both reactions is similar, which proves that the reaction on-chip is complete; excluding the possibility that the reaction has stopped because of enzyme inactivation.

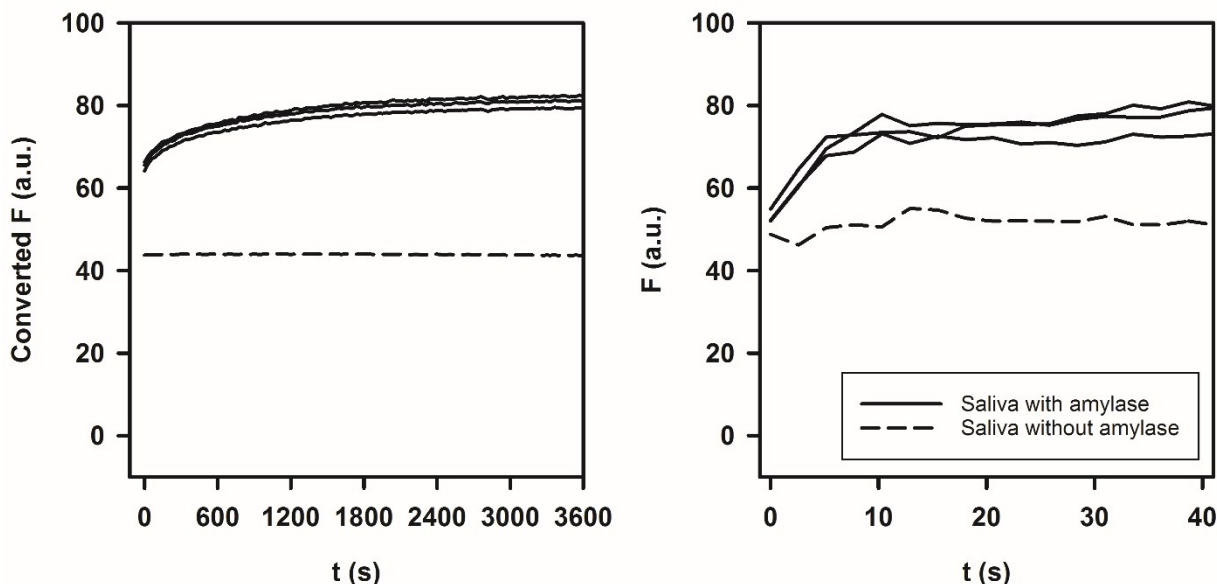


Figure S 8. Fluorescence signals from the fluorimeter-monitored digestion of labeled starch (500 $\mu\text{g}/\text{mL}$ in syringe) by α -amylase in artificial saliva (data from Figure S 5) were converted to equivalent on-chip fluorescence values to allow for a comparison between on-plate (left graph) and on-chip (right) reactions. The Y-axes are the same; the timescale of the reaction on chip (X-axis) is much shorter. Data for the initial time points are very visible on chip, but are not recorded in the fluorimeter (due to the manner in which reagents are added together in a cuvette, and starting measurements). Note the different scales on the X-axis.

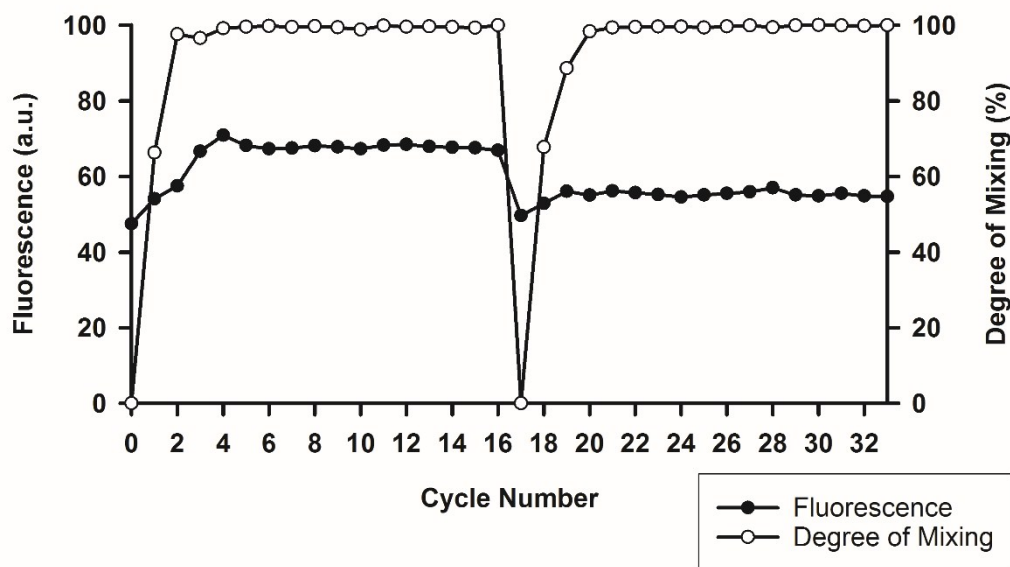


Figure S 9. Fluorescence plot of a control experiment, to monitor reaction completion: two identical micromixers were coupled in series. In the first one (cycles 0–16), saliva (11.5 U/mL α -amylase, 1.6 $\mu\text{L}/\text{min}$) was mixed with labeled, quenched starch (500 $\mu\text{g}/\text{mL}$, 0.4 $\mu\text{L}/\text{min}$). The output of this micromixer (2.0 $\mu\text{L}/\text{min}$) was transferred to the second micromixer (cycles 17–33), to which extra α -amylase solution (22.9 U/mL, in the exact same mineral composition as the oral mixture, 2.0 $\mu\text{L}/\text{min}$) was added. Fluorescence intensity (full dots) was measured before and after each cycle to monitor reaction progress. The relative standard deviation of fluorescence intensity in the same $300 \times 100 \mu\text{m}$ box was used to calculate the degree of mixing (white dots), as follows:

$$\text{Degree of Mixing (\%)} = \left(1 - \frac{SD_i - SD_{100\%}}{SD_{0\%} - SD_{100\%}} \right) \cdot 100 \%$$

In this equation, for every cycle i , and its relative standard deviation SD_i , the degree of mixing was calculated from the relative standard deviation of the first data point ($SD_{0\%}$, fully unmixed) and that of the last data point ($SD_{100\%}$, fully mixed). It can be seen that mixing is complete within two cycles of the first device, and within three cycles of the second device (which has a higher combined flow rate and thus requires a longer mixing distance).

Protease Activity in Gastric Juice (Stomach)

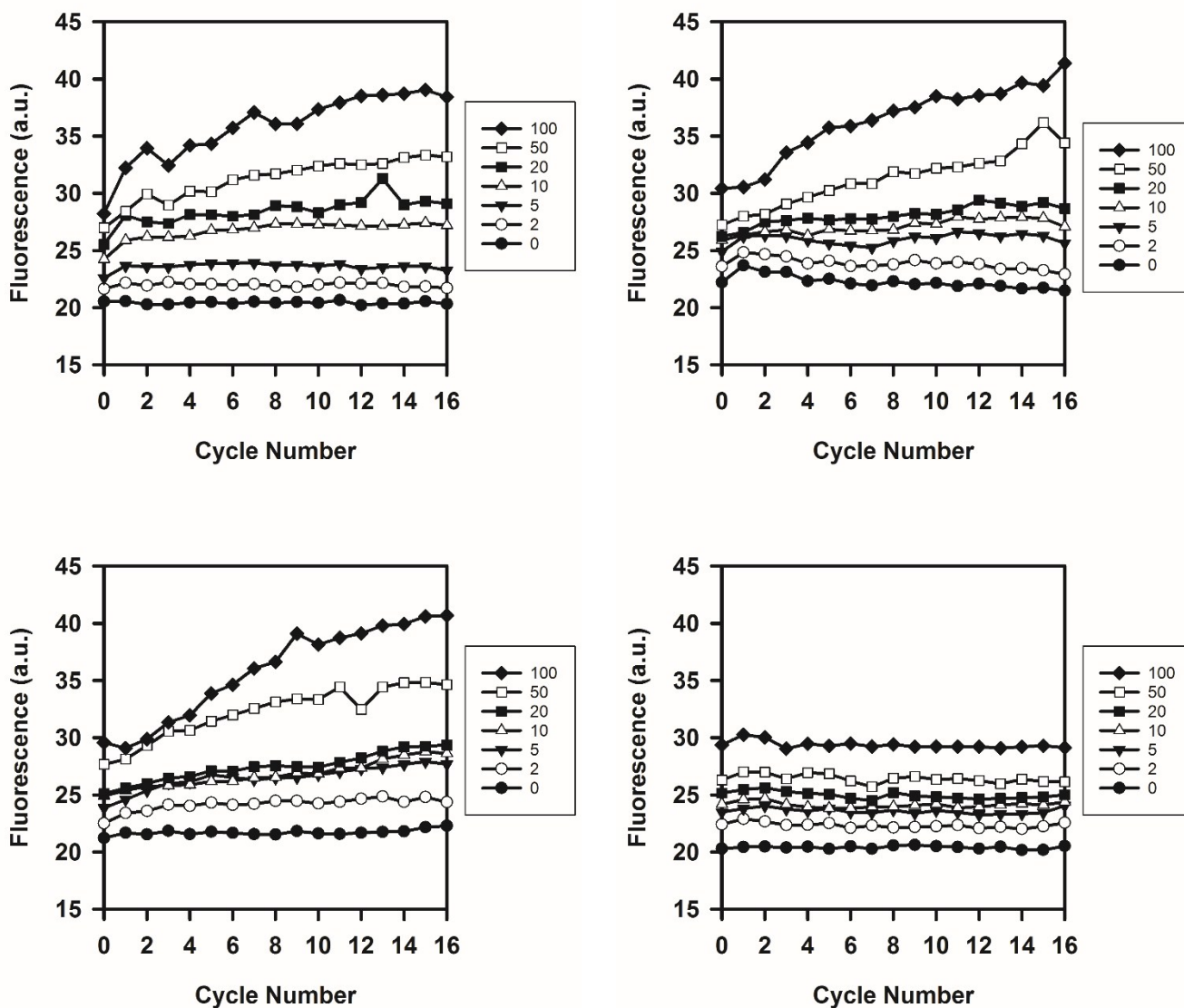


Figure S 10. On-chip fluorescence signals of the pepsin-catalyzed digestion of casein plotted against the cycle number ($n = 3$, with the negative control containing no α -amylase at the bottom right). The legend displays [casein] in the substrate inlet ($\mu\text{g/mL}$).

Protease Activity in Duodenal Juice + Bile (Intestine)

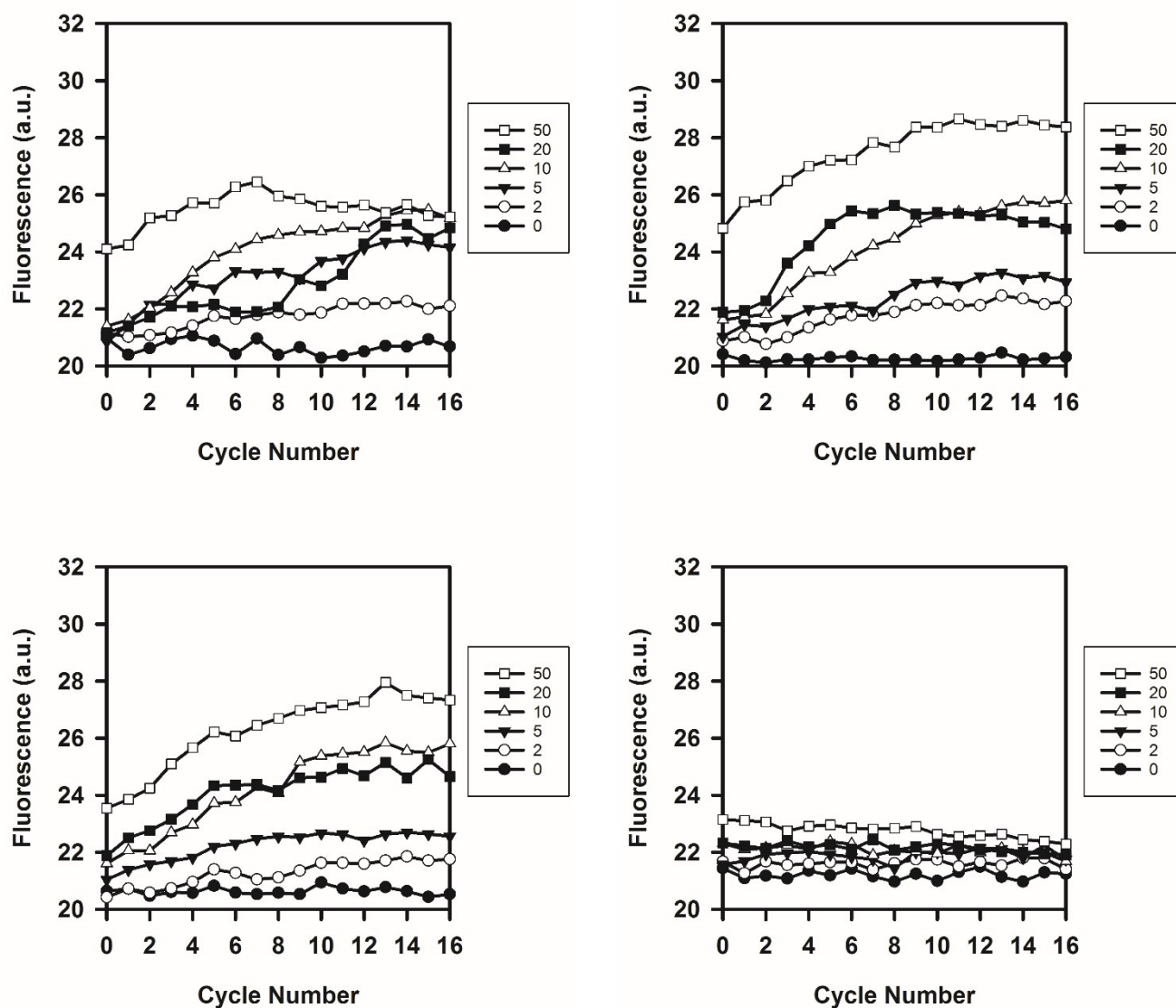


Figure S 11. On-chip fluorescence signals of the protease-catalyzed digestion of casein plotted against the cycle number ($n = 3$, with the negative control containing no α -amylase at the bottom right). The legend displays [casein] in the substrate inlet ($\mu\text{g/mL}$). Artificial duodenal juice contains pancreatin, an animal pancreas extract containing a mixture of enzymes, including proteases (e.g. trypsin).

References

- 1 M. A. Ianovska, P. P. M. F. A. Mulder and E. Verpoorte, *RSC Adv.*, 2017, **7**, 9090–9099.
- 2 D. Cutler, *J. Pharm. Pharmacol.*, 1986, **38**, 499–501.
- 3 A. P. Walczak, R. Fokkink, R. Peters, P. Tromp, Z. E. Herrera Rivera, I. M. C. M. Rietjens, P. J. M. Hendriksen and H. Bouwmeester, *Nanotoxicology*, 2013, **7**, 1198–1210.
- 4 M. Minekus, M. Alming, P. Alvito, S. Ballance, T. Bohn, C. Bourlieu, F. Carrière, R. Boutrou, F. M. Corredig, D. Dupont, F. C. Dufour, L. Egger, M. Golding, L. S. Karakaya, B. Kirkhus, S. Le Feunteun, U. Lesmes, A. Macierzanka, A. Mackie, S. Marze, D. J. McClements, O. Ménard, I. Recio, C. N. Santos, R. P. Singh, G. E. Vegarud, M. S. J. Wickham, W. Weitschies and A. Brodkorb, *Food Funct.* *Food Funct.*, 2014, **5**, 1113–1124.
- 5 D. C. Harris, *Quantitative Chemical Analysis*, W.H. Freeman and Co., New York, NY, USA, 7th Ed., 2007.

